Some observations of nonlinearly modified internal wave spectra

Hans van Haren

Royal Netherlands Institute for Sea Research, Den Burg, The Netherlands

Received 22 September 2003; revised 19 January 2004; accepted 29 January 2004; published 25 March 2004.

[1] Four examples are discussed of different internal wave band kinetic energy spectra from moored instruments at middle and high latitudes ($38° < \varphi < 61°$) in the eastern Atlantic Ocean and the western Mediterranean Sea. It is observed that for $N \gg f$, where N is the buoyancy frequency and f is the inertial frequency, the spectral falloff rate with frequency σ for internal waves tends to σ^{-3}. Either spectra are dominated at tidal and/or inertial nonlinear higher harmonics superposed on a nearly white (noise) spectral continuum, the latter extending to supertidal frequencies up to N (it is hypothesized that such a spectrum is found near the source of nonlinear interactions), or the spectrum is smooth, showing a σ^{-3} falloff rate for most of the internal wave band continuum outside an inertial peak. Such a spectrum may be typical for regions well away from the sources for interaction, although governed by the same nonlinear advection dynamics. The present observations contrast with a recently proposed model for the internal wave spectrum, similar to the canonical *Garrett and Munk* [1972] model, showing a σ^{-2} falloff rate, except for a nearly white continuum in the range between f and the solar semidiurnal tidal frequency (S_2) for latitudes $|\varphi| < 20°$. *INDEX TERMS:* 4544 Oceanography: Physical: Internal and inertial waves; 4560 Oceanography: Physical: Surface waves and tides (1255); 4508 Oceanography: Physical: Coriolis effects; *KEYWORDS:* internal waves, modifications, nonlinearity, spectra

Citation: van Haren, H. (2004), Some observations of nonlinearly modified internal wave spectra, *J. Geophys. Res.*, *109*, C03045, doi:10.1029/2003JC002136.

1. Introduction

[2] Recently, *Levine* [2002] proposed some modifications to the canonical *Garrett and Munk* [1972] (hereinafter referred to as GM) internal gravity wave frequency (σ) spectra,

$$P_{\mathrm{GM}}(\sigma) \sim N\sigma^{P}, \qquad -2.5 < p < -1.5, \tag{1}$$

between $f < \sigma < N$, where f and N are the inertial and buoyancy frequency, respectively. Amongst the modifications to the GM model were a latitudinal dependence and the treatment of vertical boundaries and turning points, namely the scale height of the vertical waveguide [*Levine*, 2002]. Another modification, considered here, concerned the energy distribution below the semidiurnal tidal frequency. On the basis of several observations [e.g., *Eriksen*, 1980; *Fu*, 1981; *Pinkel et al.*, 1987] of a whitening of the spectral continuum slope between $f < \sigma <$ the solar semidiurnal tidal frequency (S_2), *Levine* [2002] proposed a spectral frequency dependency:

$$P_L(\sigma) \sim \hat{B}(\sigma) = \frac{\pi}{2}\frac{B_{\mathrm{GM}}(\sigma)}{C} \cdot \begin{cases} 1 & \sigma_{S_2}\sigma \\ \left(1+\dfrac{f}{\sigma_{S_2}}\right)\dfrac{(\sigma/\sigma_{S_2})^3}{(\sigma/\sigma_{S_2})^{2.5}+(f/\sigma_{S_2})} & f < \sigma_{S_2} < \sigma \end{cases}, \tag{2}$$

where

$$B_{\mathrm{GM}}(\sigma) = \frac{2}{\pi}\frac{f}{\sigma(\sigma^2 - f^2)^{0.5}},$$

and where

$$C = \arccos\frac{f}{N_{\mathrm{ref}}} - \arccos\frac{f}{\sigma_{S_2}}$$

to remove f dependency of energy levels at $\sigma > \sigma_{S_2}$, where N_{ref} is a frequency associated with a reference density. This empirical model [*Levine*, 2002, Figure 3] showed strong deviations from the GM spectral slope at subtidal frequencies for near-equatorial latitudes ($|\varphi| < 20°$). *Levine* [2002] suggested that there may be dynamical reasons for this flattening in spectral slope, suggesting the tide as an energy source for the internal wave continuum. However, for midlatitudes, *Levine*'s [2002] model (2) was nearly indistinguishable from the GM model (1), and both models described mid-Atlantic Bight data equally well, except for some high-frequency (>20 cpd (one cycle per day = $2\pi/86{,}400$ s^{-1})) motions that *Levine* [2002] attributed to (unspecified) nonlinear effects.

[3] In this paper, several examples of moored kinetic energy spectra are discussed from middle and high-latitude observations that stress the need for further investigations of nonlinear interactions amongst internal gravity waves. Following recent observations [*Pinkel et al.*, 1987; *Mihaly et al.*, 1998; *van Haren et al.*, 1999, 2002], the internal wave

0148-0227/04/2003JC002136$09.00

Table 1. Moored Current Meter Data[a]

	Site[b]			
	BBA	BB8	Med	FS
Position (north)	48°03.8′	45°48.0′	38°27.2′	61°00.8′
Position (east/west)	−8°19.9′	−6°50.1′	7°33.0′	−3°19.5′
Bottom slope, deg	4.9	<0.1	∼0	1.8
Water depth, m	850	4810	2800	1043
Record depth, m	825	3810	100	1035
Instrument[c]	600 kHz ADCP	RCM-8	RCM-7	RCM-8
Interval, s	30	1200	3600	600
Period, days	22	333	129	144
Maximum speed, m s^{-1}	0.74	0.13	0.60	0.76
Local N, cpd	28 ± 10	7^{+3}_{-1}	200 ± 50	2 ± 2

[a]Frequency is calculated in cycles per day (1 cpd = $2\pi/86{,}400$ s^{-1}).
[b]BBA, Bay of Biscay (continental slope); BB8, Bay of Biscay (abyssal plain); Med, western Mediterranean Sea; FS, Faeroe-Shetland Channel.
[c]The acoustic Doppler current profiler (ADCP) is manufactured by RDI; the RCM-7 and RCM-8 are manufactured by Aanderaa.

band is not always a smooth broadband spectrum, but it can be dominated by nonlinear interactions (coupling) between near-inertial and/or semidiurnal tidal motions. Enhanced energy at interaction frequencies can, for example, result from the advection of momentum (the $\mathbf{u} \cdot \nabla\mathbf{u}$ in the momentum equations), a well-known important source for tidal higher harmonics in shelf seas [*Pingree and Maddock*, 1978]. Numerical modeling [*Xing and Davies*, 2002] has shown that the (vertical component of) nonlinear advection terms, involving the vertical internal tide velocity and the inertial shear at the level of the thermocline [*Davies and Xing*, 2003], are the dominant source of inertial-tidal interactions near the shelf edge. There nonhydrostatic effects and resulting solitons and cascades of energy to shorter wavelengths are likely to be important to resulting wave breaking.

[4] Such nonlinear internal wave motions result in different spectral slopes than do models (1) and (2) for $S_2 < \sigma <$ N; for example, *van Haren et al.* [2002] proposed a slope $p = -3$ for internal waves dominated by higher harmonics as a result of nonlinear advection. In the present paper the whitening of the (background) continuum is also investigated. As shown in section 3, the spectral falloff rate of this continuum may be observed between σ^0 and σ^{-2} in a range $\sim 0.1f < \sigma < \sim 0.5N$ ($N \gg f$), apparently independent of latitude and certainly not restricted to $|\varphi| < 20°$ and $f < \sigma < S_2$. No spectral gap is observed at frequencies just below f in the continuum.

2. Data, Sites, and Methods

[5] Currents were evaluated from four moorings deployed at various nonequatorial latitudes (Table 1, Figure 1). The observations were from near-bottom deployments (instruments at ∼30 m above the bottom) above the continental slope (Bay of Biscay (BBA) and Faeroe-Shetland Channel (FS)), from a site deep and far from the bottom of the abyssal Bay of Biscay (BB8) and from the near-surface layer above the abyssal plain of the western Mediterranean Sea (Med). Maximum current speeds were relatively high (>0.5 m s^{-1}) and comparable for three of the four sites, except for the weaker currents at BB8. However, the spectral character was quite different for all four sites due to different environmental conditions.

[6] Above the rugged, canyon-like upper continental slope in the Bay of Biscay the motions were dominated by the semidiurnal tide. Near-inertial motions were weak. The latter were also weak in the near-bottom boundary layer above the smooth continental slope in the Faeroe-Shetland Channel. There tidal motions were less than half the size of those at BBA, but subinertial motions were relatively strong, resulting in similar maximum currents. Subinertial motions were moderately strong in the Med, while tidal motions were negligibly small and near-inertial motions were relatively strong, being slightly larger than the tidal motions at FS. At BB8, inertial and tidal motions were nearly equally large, albeit smaller than at any of the previous sites. Subinertial motions were about equal in magnitude as the inertial/tidal motions, being confined to low frequencies (0.01–0.02 cpd).

[7] Moorings consisted of different types of mechanical and acoustic current meters. Owing to the relatively high current speeds and the relatively large amount of scatterers near the bottom above the upper continental slope, no instrumental defects were found to affect the records from the mechanical current meters (RCM-7 and RCM-8) and the acoustic Doppler current profiler (ADCP), respectively. The weaker currents at BB8 did not introduce substantial instrumental errors to the RCM-8 data, as was verified after comparison with a test spectral model using artificial data and records from the more energetic regions higher up the continental slope [*van Haren*, 2004a]. The bottom-mounted ADCP at BBA returned good data between 4.9 and 47.9 m above the bottom at 1 m intervals (bins). Here only one bin near the middle of the range is analyzed. The instruments sampled relatively fast (Table 1), generally resolving frequencies beyond local N, except for the

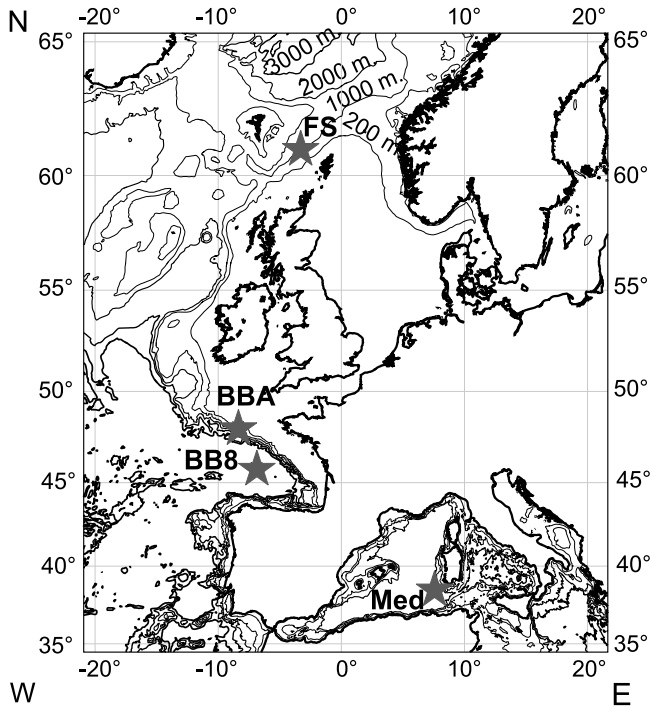

Figure 1. Map showing the different mooring locations (Table 1).

hourly sampling Med instruments. Local "background" N was estimated from conductivity-temperature-depth (CTD) profiles obtained within 5 km from each mooring just before their recovery. Table 1 reflects relative large variations in background N at each of the sites. These variations were due to uncertainty in appropriate vertical length scales and to observed temporal changes between the various CTD profiles. These spatial and temporal variations in background conditions were expected to influence the internal wave spectrum, especially at higher (supertidal) frequencies. Any variation in N (1) results in a variation in internal wave energy following GM, (2) results in a variation of the free wave frequency range, (3) results in a change in the direction of propagation of internal wave energy, and (4) is (part of) the cause of internal wave intermittency [*van Haren*, 2004b].

[8] In the spectral analysis performed here, variable smoothing was applied: $\nu \approx 3-100$ degrees of freedom (df). In order to examine spectral details, only a single cosine-bell shaped taper window was used over the entire length of the time series without further smoothing ($\nu \approx 3$ df). This weak smoothing resulted in an effective fundamental bandwidth $\delta\sigma_e \approx 2.2\delta\sigma_{fbw}$, with $\delta\sigma_{fbw}$ denoting the resolved fundamental bandwidth (~0.03 cpd for a 1 month record). Such nearly raw spectra are useful for some (e.g., tidal) motions that are deterministic rather than a particular realization of a stochastic process. Heavier smoothing was achieved by applying the same taper window over half-overlapping subsections of the time series.

[9] The observed horizontal currents were used to perform two types of spectral analysis. Kinetic energy spectra,

$$P_{KE}(\sigma) = P_{-}(\sigma) + P_{+}(\sigma), \tag{3}$$

were the sum of the rotary current component spectra $P_{-}(\sigma)$, the clockwise spectrum, and $P_{+}(\sigma)$, the anticlockwise spectrum [*Gonella*, 1972]. In the (semi) diurnal tidal band, these spectra also contained barotropic (surface wave) kinetic energy. This energy was not removed here since it involved only a few constituent frequencies in the internal wave band and because a second method was used to demonstrate the (internal) wave character of motions within the frequency band $f < \sigma < N$ using the difference of the rotary spectra. This difference was a measure for the horizontal current ellipse surface and polarization, for which *Gonella* [1972] introduced the "rotary coefficient":

$$C_R(\sigma) = (P_{-}(\sigma) - P_{+}(\sigma))/P_{KE}(\sigma). \tag{4}$$

C_R was equal to zero for purely rectilinear motion and equal to 1 for purely circular motion, its sign indicating the direction in which the ellipse was traversed. Under symmetric forcing (equal for both rotary components) and neglecting frictional stresses the solution of equation (4) became

$$C_R(\sigma) = \frac{2\sigma f}{\sigma^2 + f^2}. \tag{5}$$

At frequencies within the internal wave band, the solution of equation (5) describes free waves. It is easy to show that

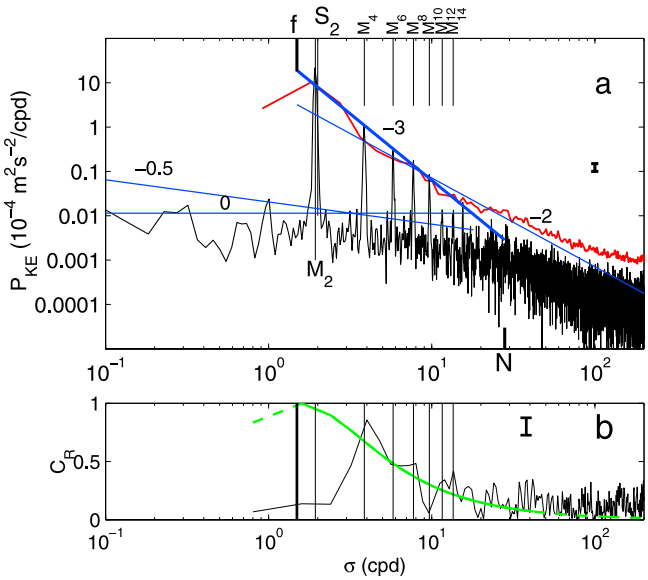

Figure 2. (a) Nearly raw ($\nu \approx 3$ degrees of freedom (df)) (black spectrum) and moderately smoothed kinetic energy spectrum ($\nu \approx 60$ df; used to compute the 95% confidence interval) (red spectrum, slightly offset in the vertical for clarity) from 22 days of acoustic Doppler current profiler (ADCP) observations at 825 m (25 m above the bottom of the continental slope) in the Bay of Biscay (BBA) (Table 1). Several spectral slopes with frequency are indicated in blue and by (p =) 0, −0.5, −2, and −3. (b) Moderately smoothed ($\nu \approx 70$ df) rotary coefficient $C_R(\sigma)$ as in equation (4), with theory (5) in green. The latter is solid within internal wave band range $f < \sigma < N + 1$ SD and dashed for other resolved spectral frequencies.

under asymmetric forcing the model for C_R is no longer sign-independent, becoming more complicated with dependence on the (different) rotary forcing components. For increasing frequencies, as $\sigma \rightarrow N$, the near-rectilinear motions may be viewed as circular motions in a plane tilted progressively stronger from the horizontal. In section 3 the C_R spectra will be used as an indicator for internal wave polarization to discriminate between (free or forced) internal waves and other "internal wave band motions."

3. Observations

3.1. Bay of Biscay (BBA)

[10] Kinetic energy spectra in the bottom boundary layer above the continental slope in the Bay of Biscay consisted of high energy at semidiurnal tidal frequencies and very little near-inertial energy (Figure 2a). In addition, within the internal wave band, conspicuous peaks were observed at higher tidal harmonic frequencies, evidence of strongly nonlinear wave profiles in the time series [*Gemmrich and van Haren*, 2001]. The strong nonlinear tidal flow field was associated with internal waves propagating obliquely downslope, thereby periodically generating gravitationally unstable stratification. The tidal harmonics were dominated by the lunar semidiurnal components M_2, M_4, M_6, ..., with amplitudes of 34.4, 6.5, 4.1 cm s^{-1}, ..., respectively, which were distinguishable from the much weaker S_2, S_4,

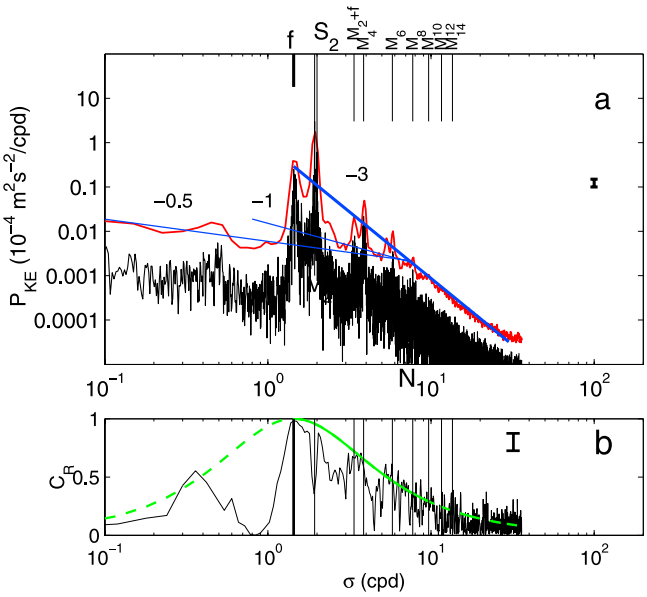

Figure 3. As in Figure 2, but for 333 days of current meter observations at 3810 m (1000 m above the bottom) in the abyssal Bay of Biscay (BB8) (Table 1).

S_6, . . ., components with amplitudes of 4.5, 1.2, 1.3 cm s^{-1}, . . ., respectively, in the nearly raw spectra, despite the short length (22 days) of the record. The lunar tidal harmonics were superposed on a nearly white ($\sim\sigma^p$, $-0.5 < p < 0$) continuum spectrum up to frequencies $\sim N \gg \sigma_{S_2}$, well beyond the cutoff proposed in model (2). In contrast with the spectral slope of the continuum, the tidal harmonic peaks showed an amplitude decrease of $\sim\sigma^{-3}$ with frequency. Because of the dominance of the tidal harmonics, the smoothed (red) spectrum had a slope $p \sim -2$ for $f < \sigma < \sim N$ before slowly decreasing its slope magnitude.

[11] The rotary coefficient spectrum (Figure 2b) demonstrated that semidiurnal tidal motions were near-rectilinear and not associated with internal gravity waves. However, the higher tidal harmonics dominating the supertidal internal wave frequencies resembled the internal wave polarization of equation (5). A more raw spectrum than displayed in Figure 2b showed that motions at the (approximately white) continuum frequencies between the (even) higher tidal harmonics and comprising nonsignificant odd harmonics did not represent internal waves as their polarization was near-rectilinear. Hypothesizing, this "internal wave band noise" could be associated with bottom boundary layer processes like variable mixing or with asymmetric forcing [*van Haren*, 2003]. However, such a continuum was also found far from the bottom at BB8 (section 3.2) and was not found in the bottom boundary layer of the Faeroe-Shetland Channel (section 3.3).

3.2. Abyssal Bay of Biscay (BB8)

[12] At 1000 m above the abyssal Bay of Biscay, ~100 km from the foot of the continental slope, nearly equally large inertial and tidal motions were observed, resulting in enhanced kinetic energy at inertial/tidal and higher tidal harmonics (Figure 3a). These spectral peaks decreased their magnitude with frequency at a rate of $\sim\sigma^{-3}$ or faster. They were superposed on a continuum having a slope $-1 < p < -0.5$ up to ~N, being about half a decade less energetic than at BBA. Also, in contrast with the observations at BBA, the total amplitude of M_2 was marginally larger than that of S_2 at BB8 ($|U|_{S_2} > 0.5|U|_{M_2}$), largely due to an amplitude change in barotropic currents, which are proportional to water depth, to first order.

[13] At BB8 and BBA the M_2 motions were rectilinear, evidence of dominant barotropic motions, but at BB8 S_2 motions showed a polarization, as expected from theory (5) (Figure 4b). As near-inertial motions also accommodated the internal wave polarization of equation (5), it was not surprising that motions at inertial-tidal and tidal-tidal interaction frequencies followed equation (5) [*van Haren*, 2003]. This implied that the latter motions were (nonlinear) internal waves. Motions at (background) continuum frequencies outside the bands of nonlinear sum-interaction frequencies and comprising nonlinear difference (backward cascade) interaction frequencies (like $M_4 - f$) as well as odd tidal harmonics showed significantly less polarization than predicted by equation (5). The kinetic energy at these "continuum" (apparently approximately white noise) frequencies was not due to an instrumental error as possible errors due to the stalling of a mechanical current meter were at least 1 decade below observations at these frequencies, as was demonstrated using a truncation model [*van Haren*, 2004a]. Apparently, at BB8, some but not all internal wave energy was transferred from (nonlinear) internal waves to these continuum frequencies but not quite as much as required to dominate random (asymmetrically forced) motions [*van Haren*, 2003]. Internal wave dominance will be observed at continuum frequencies in the Med data (section 3.4).

3.3. Faeroe-Shetland Channel (FS)

[14] In contrast with the BB-data, kinetic energy spectra from observations in weak stratification near the bottom above the continental slope in the Faeroe-Shetland Channel

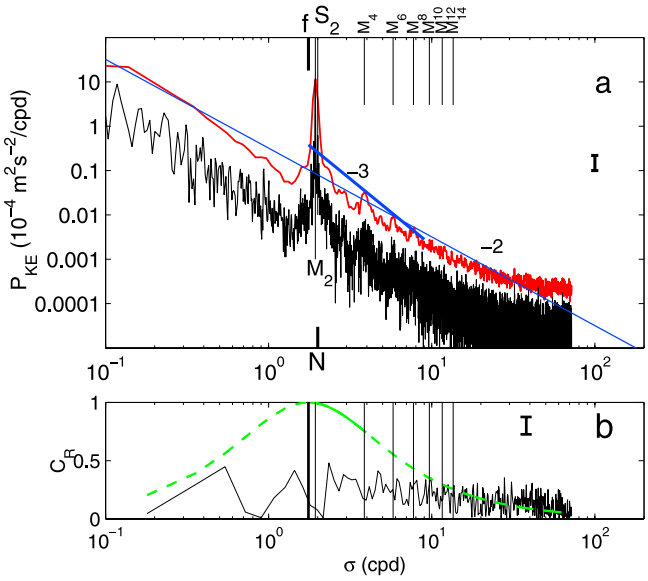

Figure 4. As in Figure 2, but for 144 days of current meter observations at 1035 m (8 m above the bottom) in the Faeroe-Shetland Channel (FS) (Table 1).

showed a $\sim\sigma^{-2}$ falloff rate of the continuum internal wave band, which extended uninterrupted to $\sigma \sim 0.1$f, except for the tidal peak (Figure 4a). Dominant motions at M_2 were about 3 times as energetic as S_2 and N_2. Higher tidal harmonics bands seemed rather broad, and they were much less energetic than in the Bay of Biscay. These higher tidal harmonics bands were also relatively flatter (less peaked) than the semidiurnal tidal band, which implied that nonlinear advection between internal tides was more important than (quasi-) linear advection by the known barotropic tidal motions. Although (quasi-) linear advection may principally result in amplitude increase (just like nonlinear advection) following parametric excitation, its spectral result is not commensurate with the present observations. As the barotropic tidal current is dominated at a single harmonic constituent (M_2), (quasi-) linear advection would yield higher harmonics bands peaking at deterministic frequencies M_4, M_6,... This is contrary to the present observations. In the FS the higher harmonics barely exceeded the red continuum. Nevertheless, their (statistically insignificant) "peaks" showed a $p \sim -2.5$ slope, slightly steeper than the continuum but less steep than observed above.

[15] Despite these spectral slopes in the kinetic energy spectra, the near-bottom FS motions were not dominated by (linear or nonlinear) internal waves (Figure 4b). Only a very weak elevation of polarization was observed in the band between semidiurnal and fourth-diurnal frequencies. The observed near-rectilinear dominancy suggested fine structure contamination by frontal passages delineating stratified and well-mixed waters, which can result in a $\sim\sigma^{-2}$ falloff rate [*Phillips*, 1971; *Reid*, 1971]. The presented observations did not differ much from 75 kHz ADCP observations at 200 m above the bottom at 850 m in the FS (N = 7 ± 5 cpd). These observations showed a slightly steeper spectral continuum slope, otherwise being featureless, and a slightly more enhanced polarization between 1f and 3f, albeit significantly less than equation (5). Apparently, the observations in Figure 4 are typical for the strongly varying (stratification) conditions at depths outside the depth (~500 m) of the main pycnocline in the Faeroe-Shetland Channel, resulting in frequent passages of layers of $N \sim 0$ that (spectrally) dominate internal waves. In contrast, similarly featureless kinetic energy spectra having approximately the same spectral slope as FS, but that did show dominant internal wave polarization, were observed in the Med.

3.4. Western Mediterranean Sea (Med)

[16] In contrast with the FS data, kinetic energy spectra in the strongly stratified layer near the surface above the abyssal Algerian Basin, western Mediterranean Sea, showed a $p = -2.9 \pm 0.2$ slope of the continuum between $1.3f < \sigma < 3f$, which was elevated above a general slope of $p \approx -2$ from $\sim 0.1f < \sigma < 10f$ (Figure 5a). The Med spectrum was representative of the canonical GM spectrum in its smoothness with the single peak near f but not in its continuum slope. Tides were less energetic than the continuum. No significant higher inertial harmonics were observed. Nevertheless, the continuum consisted of smoothly distributed internal wave energy, as was inferred from the rotation coefficient spectrum (Figure 5b), with observations significantly confirming equation (5). These observations of a $p \sim -3$ slope suggested nonlinear interactions transferring energy to a much higher number of different frequencies than in the tidally dominated BBA or the inertial-tidally dominated BB8.

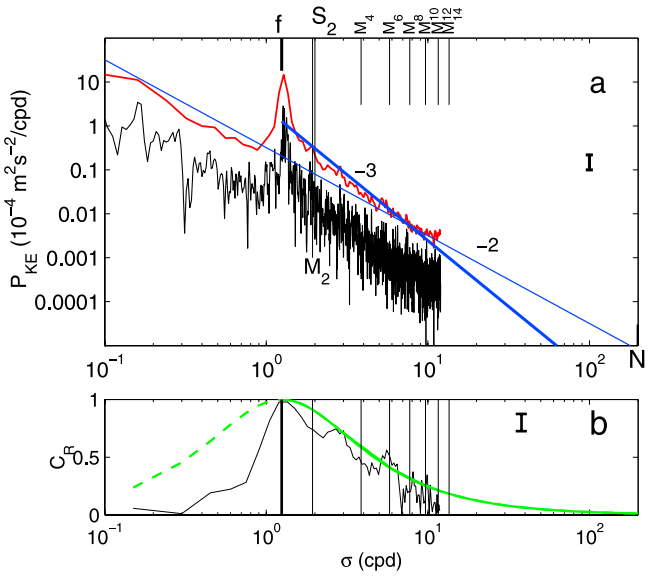

Figure 5. As in Figure 2, but for 129 days of current meter observations at 100 m (2700 m above the bottom) in the Algerian Basin, western Mediterannean Sea (Med) (Table 1), during a period without passage of mesoscale eddies so that the top of the mooring moved <10 m vertically.

4. Discussion

[17] Previous [e.g., *Fu*, 1981] and the present observations show differences to the smooth model spectra (1) and (2) for specific ocean areas: Internal wave band spectra do not always display a $p = -2$ spectral slope for $\sigma > S_2$, and local differences may be more important than latitudinal dependence. This holds for the "internal wave band continuum" ($-1 < p < 0$) as well as for a smoothed version of internal wave spectra dominated by nonlinear interactions ($p = -3$).

[18] In the case of a smoothed spectrum, the spectral slope depends either on the amount of inertial/semidiurnal tidal energy and the associated energy at their interaction frequencies [*van Haren et al.*, 2002] (BBA and BB8 in this paper) or on the amount of near-inertial energy and stratification (Med). When sufficient stratification and sufficient near-inertial energy are available, a slope $p = -3$ results for the first half decade of the internal wave band ($\sim 1.3f < \sigma < \sim 3-5f$). Following suggestions by *van Haren et al.* [2002], this is a typical spectral slope for strong nonlinear interactions, which can also smoothly fill an entire internal wave band spectrum from just a single source (at f), as in two-dimensional subinertial range turbulence [*Thompson*, 1971]. Given the observations in the Mediterranean Sea and the Bay of Biscay, one could hypothesize that the difference between these spectra is evidence of the distance to the source of nonlinear interactions. Apparently, this determines the level of second-order and higher-order internal wave interactions that eventually change the spectral slope of the continuum from $p = 0$ near the source (BBA) to $p = -3$

(Med) "far" from it. In between, an area dominated by (strongly nonlinear) frontal passages leads to $p = -2$ (FS). Alternatively, the lack of enhanced subinertial energy at the BBA site may contribute to a lack of energy distribution to continuum frequencies around the tidal harmonics peaks. Compared to BB8, progressively more subtidal energy at BB8 and even more at Med may have facilitated the spectral (re-) distribution or enhanced spectral smoothing, especially in the latter (and, differently, also in the FS).

[19] In the Bay of Biscay the observed reduced energy redistribution outside inertial/tidal harmonics, resulting in the $-1 < p < 0$ sloping continuum, demonstrates that internal wave energy can reside at distinct frequencies. Such low continuum-slope magnitudes were reported previously as being typical for the anticlockwise rotary current component [*Pinkel et al.*, 1987]. As this component is usually much weaker than the clockwise component for internal waves, the observed slopes p confirm our observations that the motions outside the tidal and inertial-tidal harmonics are evidence of weak internal waves at these frequencies, not exceeding approximately white noise levels introduced by random or asymmetrically forced internal wave band motions. The latter motions can be simply a continuation of the subinertial spectrum rather than waves. However, presently, it is not clear how to model such approximately random motions. Likewise, the precise extent of nonlinear interaction peaks above this (quasi-) random noise level is imperative for further understanding of the internal wave (band) spectrum.

[20] One could model the BBA observations by (arbitrarily) changing the frequency cutoff in the (statistical) model (2) for the transition between the near-white and red ($p \sim -2$) continua, up to $\sigma \sim$ N. However, such rather arbitrary change ignores the effects of nonlinearity at some distance from the source and the effects of nonlinearity following interactions between subinertial and internal wave band motions. Therefore it is suggested that future models incorporate the dynamics of nonlinear advection within the internal wave band, modeling shear instabilities and other nonhydrostatic effects, as, for example, in the work of *Xing and Davies* [2002] and *Davies and Xing* [2003], and include interactions with varying background conditions. Present models like those of *Levine* [2002] and *Xing and Davies* [2002] should stimulate further progress on the understanding of waves in the ocean interior.

[21] **Acknowledgments.** I thank the crew of the *Pelagia* for assistance during deployment and recovery of all moorings. I gratefully acknowledge the support of Claude Millot (Antenne LOB-COM-CNRS, c/o IFREMER, France) for the use of Mediterranean Sea data. I thank IFREMER for the hospitality during a short stay in La Seyne-sur-mer, which was generously supported by a grant from the Netherlands organization for the advancement of scientific research, NWO, in the French-Dutch exchange program. The "TripleB" project in the Bay of Biscay (Hendrik van Aken) and the PROCS project in the Faeroe-Shetland Channel were also supported by grants from NWO.

References

Davies, A. M., and J. Xing (2003), On the interaction between internal tides and wind-induced near-inertial currents at the shelf edge, *J. Geophys. Res.*, *108*(C3), 3099, doi:10.1029/2002JC001375.

Eriksen, C. C. (1980), Evidence for a continuous spectrum of equatorial waves in the Indian Ocean, *J. Geophys. Res.*, *85*, 3285–3303.

Fu, L.-L. (1981), Observations and models of inertial waves in the deep ocean, *Rev. Geophys.*, *19*, 141–170.

Garrett, C. J. R., and W. H. Munk (1972), Space-time scales of internal waves, *Geophys. Fluid Dyn.*, *3*, 225–264.

Gemmrich, J. R., and H. van Haren (2001), Thermal fronts generated by internal waves propagating obliquely along the continental slope, *J. Phys. Oceanogr.*, *31*, 649–655.

Gonella, J. (1972), A rotary-component method for analysing meteorological and oceanographic vector time series, *Deep Sea Res.*, *19*, 833–846.

Levine, M. D. (2002), A modification of the Garrett-Munk internal wave spectrum, *J. Phys. Oceanogr.*, *32*, 3166–3181.

Mihaly, S. F., R. E. Thomson, and A. B. Rabinovich (1998), Evidence for non-linear interaction between internal waves of inertial and semidiurnal frequency, *Geophys. Res. Lett.*, *25*, 1205–1208.

Phillips, O. M. (1971), On spectra measured in an undulating layered medium, *J. Phys. Oceanogr.*, *1*, 1–6.

Pingree, R. D., and L. Maddock (1978), The M_4 tide in the English Channel derived from a non-linear numerical model of the M_2 tide, *Deep Sea Res.*, *26*, 53–68.

Pinkel, R., A. Plueddemann, and R. Williams (1987), Internal wave observations from FLIP in MILDEX, *J. Phys. Oceanogr.*, *17*, 1737–1757.

Reid, R. O. (1971), A special case of Phillips' general theory of sampling statistics for a layered medium, *J. Phys. Oceanogr.*, *1*, 61–62.

Thompson, R. (1971), Topographic Rossby waves at a site north of the Gulf Stream, *Deep Sea Res.*, *18*, 1–19.

van Haren, H. (2003), On the polarization of oscillatory currents in the Bay of Biscay, *J. Geophys. Res.*, *108*(C9), 3290, doi:10.1029/2002JC001736.

van Haren, H. (2004a), Incoherent internal tidal currents in the deep ocean, *Ocean Dyn.*, *54*, 66–76, doi:10.1007/s10236-003-0083-2.

van Haren, H. (2004b), Bandwidth similarity at inertial and tidal frequencies in kinetic energy spectra from the Bay of Biscay, *Deep Sea Res., Part I*, in press.

van Haren, H., L. Maas, J. T. F. Zimmerman, H. Ridderinkhof, and H. Malschaert (1999), Strong inertial currents and marginal internal wave stability in the central North Sea, *Geophys. Res. Lett.*, *26*, 2993–2996.

van Haren, H., L. Maas, and H. van Aken (2002), On the nature of internal wave spectra near a continental slope, *Geophys. Res. Lett.*, *29*(12), 1615, doi:10.1029/2001GL014341.

Xing, J., and A. M. Davies (2002), Processes influencing the non-linear interaction between inertial oscillations, near inertial internal waves and internal tides, *Geophys. Res. Lett.*, *29*(5), 1067, doi:10.1029/2001GL014199.

H. van Haren, Royal Netherlands Institute for Sea Research, P.O. Box 59, 1790 AB Den Burg, The Netherlands. (hansvh@nioz.nl)